

Light and scanning electron microscopic examination of the Saanen goat heart

Sedef SELVİLER SİZER^{1*}, Yonca Betil KABAK², Murat KABAK¹

¹Department of Anatomy, Faculty of Veterinary Medicine, Ondokuz Mayıs University, Samsun, Turkey

²Department of Pathology, Faculty of Veterinary Medicine, Ondokuz Mayıs University, Samsun, Turkey

Received: 29.05.2020 • Accepted/Published Online: 27.09.2020 • Final Version: 18.12.2020

Abstract: It is important to know the morphological structure of the heart, which is a vital organ of the body, in detail. For this reason, we aimed to examine the morphological structure of the Saanen goat heart using light and scanning electron microscopy (SEM). A total of thirteen Saanen goat hearts were used in the study. To demonstrate the histological structure of the heart, samples taken from 9 hearts were fixed in 10% formaldehyde solution and blocked in paraffin after routine histological procedures. Histological staining was performed on the sections taken from the blocks. Four hearts were fixed in a 2.5% glutaraldehyde solution for electron microscopic examination. The samples taken were dehydrated with different concentrations of acetone, treated with osmium tetroxide, and critical point dried in accordance with SEM procedures. After being coated with gold/palladium (Au/Pd), samples were made ready for imaging under SEM. The general structure of the heart was determined in detail with histological and SEM examination. Although the structural findings of the Saanen goat heart were generally similar to findings in the literature, the shapes of the cells that formed the Purkinje fiber networks in SEM examination were different from other species. It is thought that the images obtained will help in studies of the morphological structure of the heart and in detecting pathological changes that may occur in the heart.

Key words: Heart, histology, Saanen goat, scanning electron microscopy

1. Introduction

The heart, a vital organ of the circulatory system, is located in the pericardium on the left side of the middle mediastinum in the thoracic cavity [1–3]. The heart wall consists of three layers: epicardium, myocardium, and endocardium [1,4–7]. The outermost layer of the heart wall is the epicardium, which is the innermost layer of the pericardium [4,6,8]. The myocardium, which is the middle layer, is the thickest of the three layers; the endocardium is the innermost layer [4,6,8]. When the structural features of the heart wall are examined, there is a specialized heart muscle for contraction, a fibrous skeleton for connecting the valves, and a specialized internal conduction system for muscle contractions [8–11].

There are many studies in which structures such as the Purkinje fibers [9,12–15], intercalated discs [16,17], ventricular myocardium [18], sinoatrial node [9,11,12,19], atrioventricular node [20–22], bundle of His [20,23], tendinous cords [24], heart muscle [4,6,25–27], and heart valves [28–32] have been examined using light or electron microscopy. One of the advantages of SEM imaging is that three-dimensional images are obtained because focusing produces images of varying depth; hence, it is widely used in many fields such as anatomy, cell biology, physiology,

pathology, microbiology, toxicology, and engineering [33,34]. It is thought that a structure examined using SEM is easier to understand and that SEM facilitates the identification of any differences that occur on its surface [33]. Therefore, SEM can be used to visualize the heart's structure in three dimensions [16].

Although there are light microscopic images of the general morphological structures of the heart, SEM study has been insufficient in this area in domestic mammals. This situation makes it difficult to recognize the structures seen in the heart in SEM examination. For this reason, our aim is to increase the recognition of tissues by revealing the morphological structures of the heart, and to assist researchers working with SEM.

2. Materials and methods

2.1. Animals

In this study, 13 hearts of Saanen goats obtained from butchered animals were used.

2.2. Histological technique

Nine of the Saanen goat hearts were fixed in 10% buffered formaldehyde solution for histological examination. Samples taken to examine the layers and internal structure

* Correspondence: sedef.selviler@omu.edu.tr

of the heart were blocked in paraffin after routine tissue follow-up procedures. Sections of 5- μ m thickness taken with a Leica microtome (RM2125RT; Leica, Wetzlar, Germany) were stained with hematoxylin–eosin (H&E), Masson's trichrome, Crossman trichrome, and orcein stain techniques [35]. Histological examination was done with a Nikon Eclipse E600W light microscope (Nikon, Tokyo, Japan), and microscopic photographs were taken with the Nikon DS Camera Head DS-5M imaging system.

2.3. Scanning electron microscopy

Four hearts were fixed in 2.5% glutaraldehyde solution for SEM examination. Samples were taken from different points of the heart. Two methods were used to examine the subepicardial and subendocardial layers. In the first method used, the endocardium and epicardium were removed under a stereomicroscope. In the second method, samples were kept in 2N-NaOH solution for 3–7 days at 25 °C. Tissues washed with distilled water were then put in tannic acid solution. All prepared samples were washed with phosphate buffer solution (PBS) according to SEM procedures. The samples were dehydrated with serial acetone dilutions and were then treated with osmium tetroxide and critical point drying. Following this, tissues covered with gold/palladium (Au/Pd) were examined in detail with SEM (GeminiSEM 500, ZEISS, Oberkochen, Germany; JSM-7001F, JEOL, Tokyo, Japan).

3. Results

3.1. Histological results

Histologically, it was observed that the heart consisted of 3 layers in all of the atria and ventricles: epicardium, myocardium, and endocardium (Figure 1a). It was determined that the outermost part of the epicardium was covered with mesothelial cells (Figure 1b). Under these cells was a thin connective tissue containing a large number of elastic fibers (Figure 1b). Below this layer, a subepicardial layer consisting of blood vessels, nerve fibers, and abundant adipose cells was observed. It was determined that the myocardium, which is the middle layer, consisted of cardiac muscle cells with a single oval-shaped nucleus and cross-striation. Intercalated discs were seen where the muscle fibers were connected (Figure 1c). It was noted that there were collateral connections between adjacent muscle fibers (Figure 1d). It was determined that the endocardium covering the innermost surface of the heart and the surface of the heart valves (Figure 2) consisted of endothelium with subendothelial and subendocardial layers. The endothelium was formed of simple squamous epithelium; the subendothelial layer consisted of loose connective tissue and smooth muscle cells (Figure 3a). The subendocardial layer, the last layer of the endocardium, was composed of loose connective tissue, nerve fibers, and Purkinje fibers. Purkinje fibers were observed to have large nuclei and light cytoplasm (Figure 3b).

3.2. SEM results

The endocardium was the inner layer of the heart and consisted of three layers. The endothelium was located in the deepest, covering the inner surface of the heart and consisted of a simple squamous epithelium (Figures 4a and 4b). The border between the second (subendothelial) and third (subendocardial) layers of the endocardium containing connective tissue was not apparent (Figures 4a and 4b). The collagen fibrils located in the subendocardial layer were thicker than those in the subendothelial layer. The subendocardial layer of the right ventricles of the macerated samples contained Purkinje strands consisting of cells of elongated form which were connected to each other (Figure 5). The subendocardial layer continued with myocardium, the muscle layer of the heart (Figures 4a and 4b). It was observed that each muscle bundle in the myocardium consisted of muscle fibers extending parallel to each other longitudinally, and that these fibers made collateral connections with each other in some regions (Figure 6a). Connection points of different appearance on the surface of the muscle fibers attracted our attention. Dark-colored A-bands and light-colored and line-shaped I-bands between the A-bands were observed (Figure 6b). Numerous mitochondria were found at the level of the A-bands of the muscle fibers. When the thickness of the myocardium was examined, it was revealed that the myocardium in the ventricles was thicker than that of the atria. Epicardium, the third layer, consisted of mesothelium, loose connective tissue (Figure 7a), and adipose tissue (Figure 7b). In addition to the heart wall, pectinate muscles and valves such as the tricuspid valve, mitral valve, and aortic valve were examined. It was determined that the pectinate muscles (Figure 8) covering the inner side of the right and left atria were of different thicknesses. It was observed that the pectinate muscles in each atrium were interconnected and had a network appearance. The mitral valve (Figure 9a), tricuspid valve (Figure 9b), and aortic valve (Figure 9c), whose surfaces were covered with endothelium and many row-shaped structures with oval-shaped, smooth borders in the surface endothelium of those, were noticeable. There were overhangs that appeared as light-colored dots on these structures (Figure 9d). It was observed that tendinous cords were attached to the mitral valve and tricuspid valve. In addition, lymphocytes, which are important in immunity and have many protrusions, were also seen (Figure 10).

4. Discussion

Heart tissue has been reported to consist of 3 layers—the epicardium, myocardium, and endocardium—in histological and electron microscopic examinations [4,6,7,36,37]. In Saanen goats, the heart consists of 3 layers in accordance with the literature. In this study,

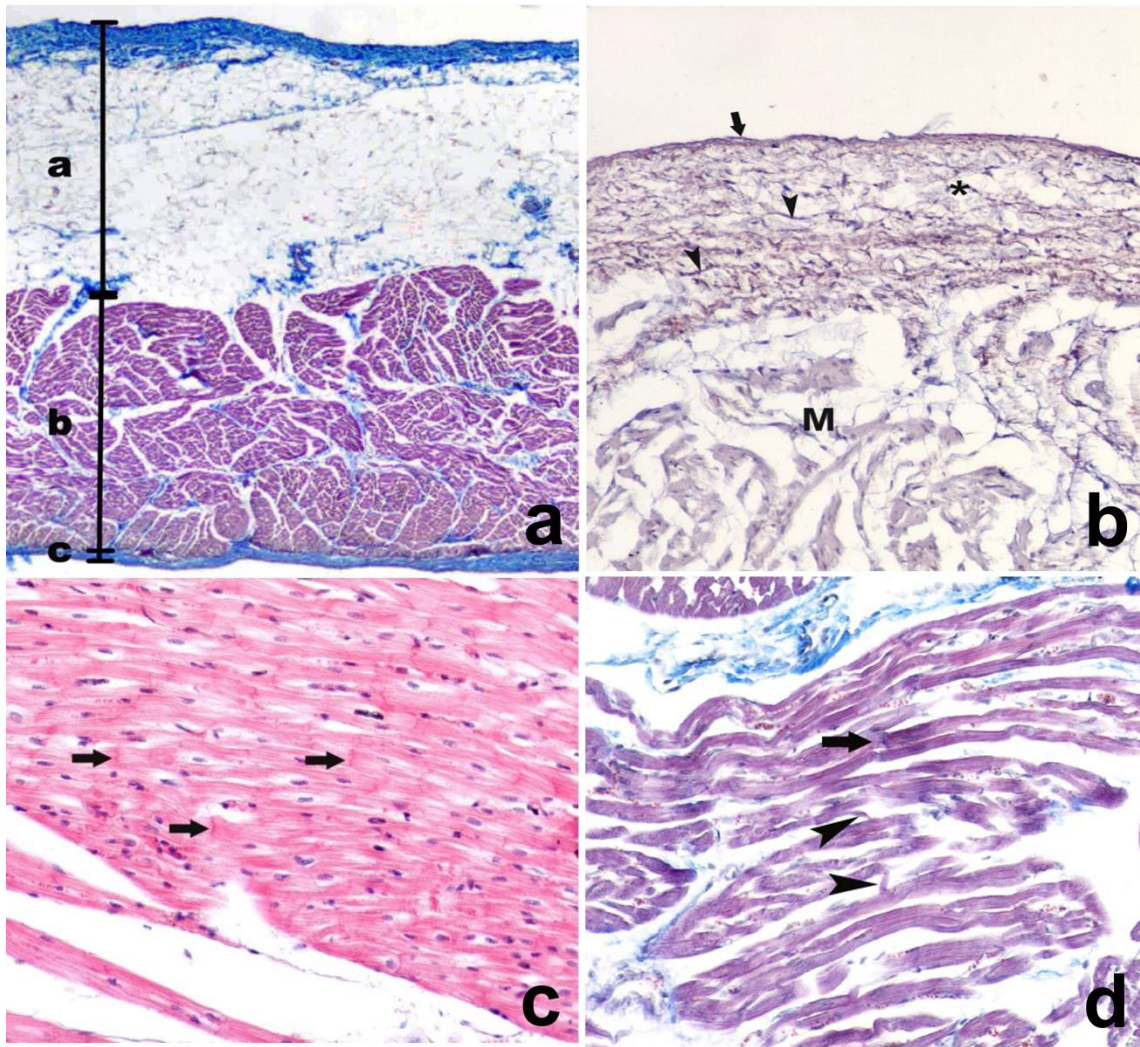


Figure 1. a: General histological view of right atrium, epicardium (a), myocardium (b), endocardium (c), 10× objective magnification, (Masson's trichrome); b: The view of epicardium and myocardium layers, mesothelial cells (arrows) in the epicardium, under this layer elastic fiber (arrowhead), connective tissue (*), and myocardium (M), 10× objective magnification, (Orcein); c: The view of the myocardium, intercalated disc (arrows), 2× objective magnification, (H&E); d: View of the myocardium, collateral connections (arrowheads), and intercalated disc (arrow), 2× objective magnification, (Crossman trichrome).

the epicardium corresponds to findings in the literature [4,6,7,36,37]. The mesothelium and subepicardial layer underneath it consisted of connective tissue, adipose tissue, and blood vessels. In the Saanen goat, the cardiac muscle cells contain a single nucleus; these cells make intercalated disc and collateral connections with each other, similar to findings in the literature by Eurell and Frappier [36] and Ross and Pawlina [8]. Myofibrils have been examined with SEM in the human [16], monkey [17], and sheep [18], and findings of the A-, I-, and Z-bands were obtained. Since the Z-bands are a very thin line within the I-bands, only A- and I-bands were identified in the myofibrils of Saanen goats. The structures of these bands were compatible with those described

in the literature [16–18]. It has been reported that the innermost layer, the endocardium, was made up of a simple squamous epithelium-containing endothelium, subendothelial layer containing fibroelastic connective tissue and smooth muscle cells, and subendocardial layer containing blood vessels and Purkinje fibers [36–38]. This situation was similar to our findings for Saanen goats. In the SEM examination, the endocardium was composed of the endothelium, with subendothelial and subendocardial layers, which is compatible with the findings of studies in humans [4,6]. The cell shapes forming the Purkinje fiber network observed in the subendocardial layer were reported to be oval in whale, sheep, and goat [14,39,40] and cylindrical in human, monkey, and dog [14], whereas

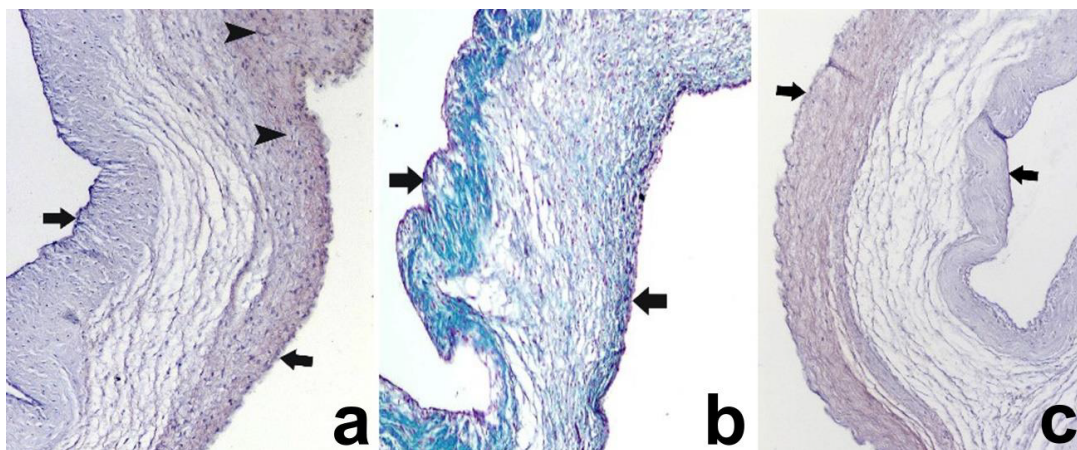


Figure 2. a: Histological view of mitral valve, endothelium (arrows), elastic fibers (arrowheads), 10× objective magnification (Orcein); b: Histological view of tricuspid valve, endothelium (arrows), 10× objective magnification (Masson's trichrome); c: Histological view of aortic valve, endothelium (arrows) 10× objective magnification (Orcein).

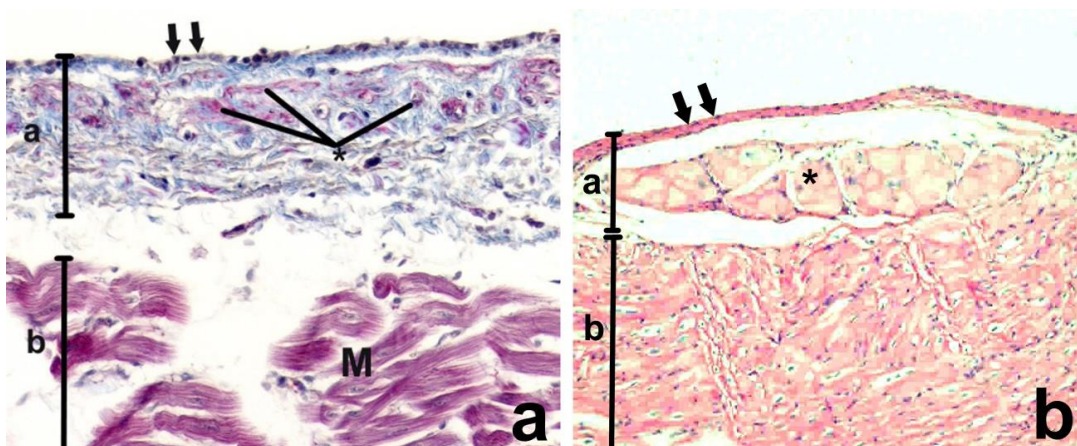


Figure 3. a: The view of the endocardium and myocardium layers, endocardium (a), endothelium (arrows), connective tissue and smooth muscle cells (*), myocardium (b) myocytes (M), 20× objective magnification, (Crossman trichrome); b: View of Purkinje fibers, endocardium (a), endothelium (arrows), purkinje cells (*) in the subendocardial layer and myocardium (b), 10× objective magnification, (H&E).

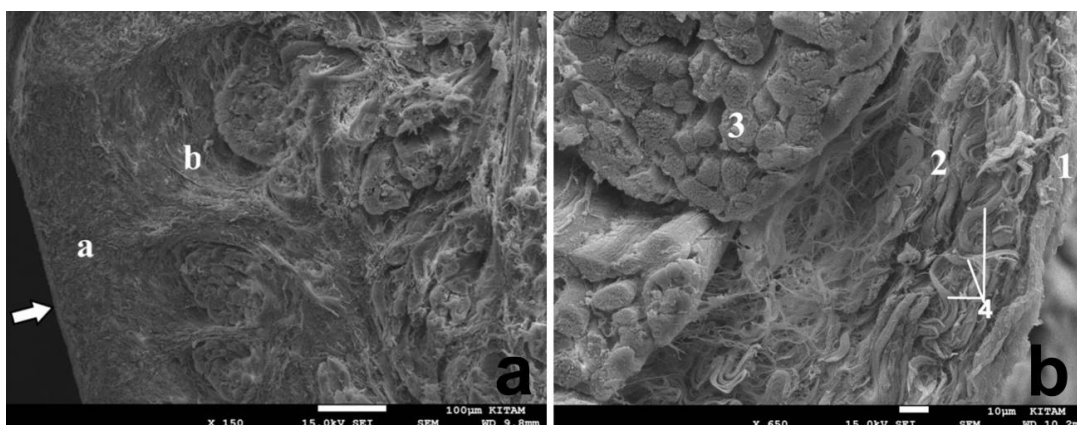


Figure 4. a: View of the left atrium, endothelium (arrow), connective tissue (subendothelial-subendocardial) (a), myocardium (b), 150×; b: The view of the right atrium, subendothelial connective tissue (1), subendocardial connective tissue (2), myocardium (3), collagen fibers (4), 450×.

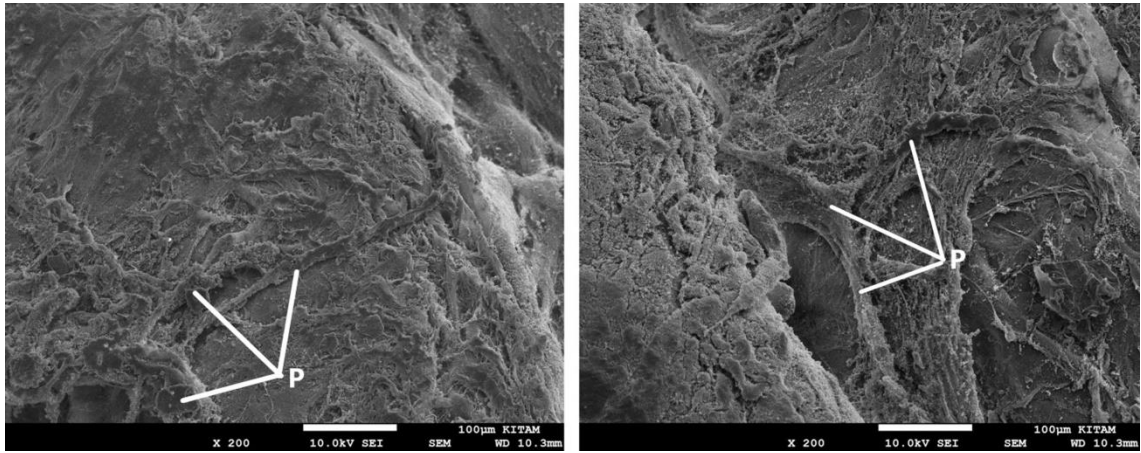


Figure 5. Purkinje networks (P) in the subendocardial layer in right ventricle, 200× (2N-NaOH maceration method).

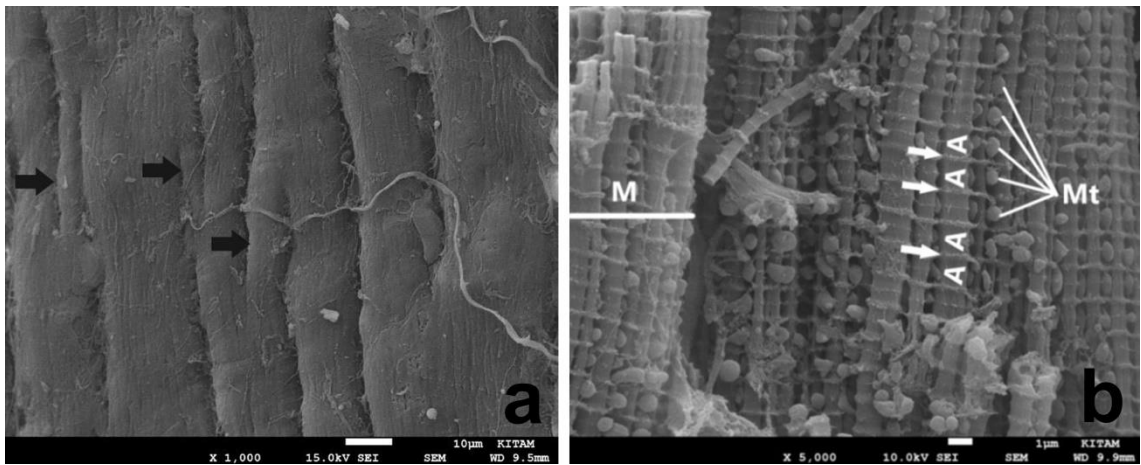


Figure 6. a: The view of muscle fibers in the myocardium in the left ventricle, collateral connection (arrows), 1000×; b: The myocardium in right ventricle A band (A), I band (arrow), mitochondria (Mt), muscle fiber (M), 5000×.

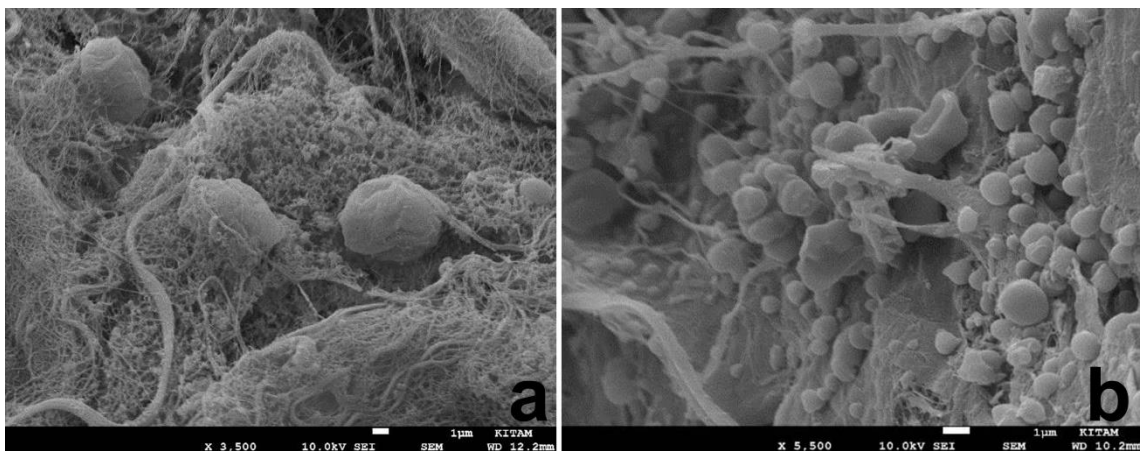


Figure 7. a: The view of collagen fibers and connective tissue in the subepicardial layer in right ventricle, 3500×; b: Adipose tissue in the subepicardial layer of right ventricle, 5500×.

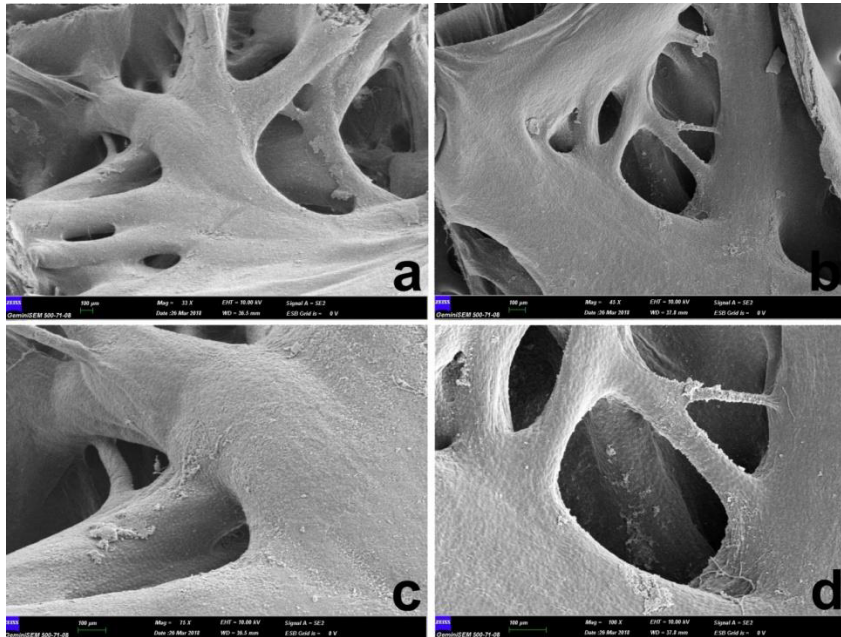


Figure 8. The view of pectinate muscles. (a) 33×, (c) 75× in the left atrium, (b) 45×, (d) 100× in the right atrium.

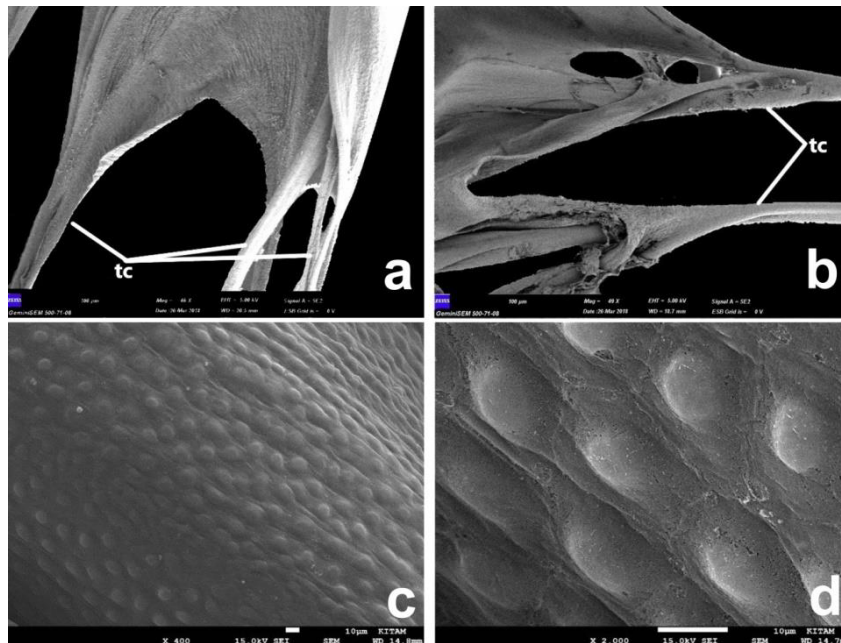


Figure 9. a: The view of mitral valve, tendinous cords (tc), 46×; b: The view of tricuspid valve, tendinous cords (tc), 49×; c: Surface view of aortic valve (septal semilunar cusp), 400×; d: Surface view of aortic valve (septal semilunar cusp), 2000×.

those of Saanen goats were observed to be elongate, similar to those reported by Canale et al. [41]. There is an SEM study in the mouse and rabbit on tricuspid, mitral, and aortic valves [42]. In this study, it was mentioned that the surfaces of the heart valves are covered with endothelium

and that there are sequential protruding structures with nanocilia over these structures [42]. These structures and their nanocilia-like protrusions were also observed on the examined heart valve surfaces of Saanen goats. We think that these protrusions seen on the endothelium

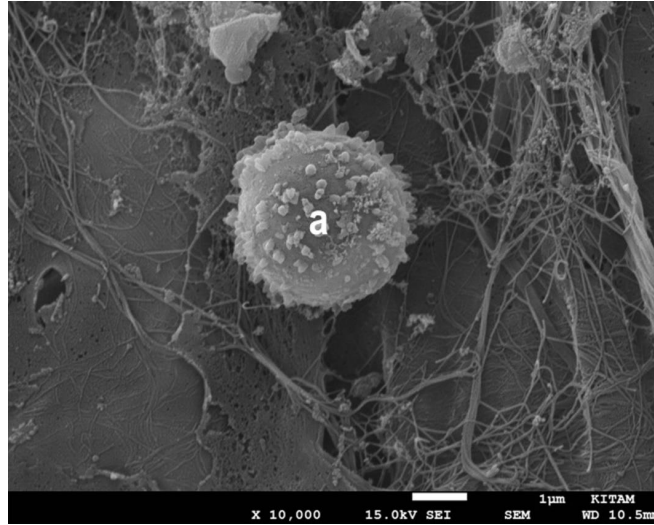


Figure 10. View of lymphocyte (a) in the left atrium, 10,000×.

are the nuclei of endothelial cells. In addition, SEM examination of T and B lymphocytes, which play a role in the immune system, have been performed in studies conducted by Polliack et al. [43] and Polliack et al. [44]. These researchers stated that the cells with a smoother surface are T lymphocytes and the cells with microvilli on their surface are B lymphocytes. During the SEM examinations we performed of the hearts of the Saanen goat, cells with many microvilli-like protrusions were found on the surface. We think that these cells are B lymphocytes.

In conclusion, histological findings of the Saanen goat heart were consistent with findings in the literature.

References

1. Dyce KM, Sack WO, Wensing CJG. Textbook of Veterinary Anatomy. 4th ed. Missouri, MO, USA: Elsevier; 2009.
2. Nickel RA, Schummer A, Seiferle E. The Anatomy of The Domestic Animals. 3th ed. Berlin, Hamburg: Verlag Paul Parey; 1981.
3. Wessels A, Sedmera D. Developmental anatomy of the heart: a tale of mice and man. *Physiological Genomics* 2003; 15 (3): 165-176. doi: 10.1152/physiolgenomics.00033.2003
4. Gálfiová P, Polák Š, Mikušová R, Gažová A, Kosnáč D et al. The three-dimensional fine structure of the human heart: a scanning electron microscopic atlas for research and education. *Biologia* 2017; 72 (12): 1521-1528. doi: 10.1515/biolog-2017-0175
5. König HE, Ruberte J, Liebich HG. Systema cardiovasculare. In: König HE, Liebich HG (editors). *Veterinary Anatomy of Domestic Mammals*. 6th ed. Stuttgart, Germany: Schattauer; 2013. pp. 450-460.
6. Varga I, Kyselovič J, Galfiova P, Danisovic L. The non-cardiomyocyte cells of the heart. their possible roles in exercise-induced cardiac regeneration and remodeling. In: Xiao J (editor). *Exercise For Cardiovascular Disease Prevention and Treatment*. vol 999. Singapore: Springer; 2017. pp. 117-136.
7. Widmaier EP, Raff H, Strang KT. *Vander's Human Physiology: The Mechanisms of Body Function*. 12th ed. New York, NY, USA: McGraw-Hill; 2011.
8. Ross MH, Pawlina W. *Histology: Text and Atlas*. 6th ed. Baltimore, MD, USA: Lippincott Williams & Wilkins; 2011.
9. Ghonimi W, Balah A, Bareedy MH, Salem HF, Soliman SM et al. Sinu-atrial node of mature dromedary camel heart (camelus dromedarius) with special emphasis on the atrial purkinje like cardiomyocytes. *Journal of Cytology and Histology* 2015; 6:3. doi: 10.4172/2157-7099.1000319

However, the cells forming the Purkinje fiber network in the Saanen goat heart seen in SEM examination had an elongated shape, unlike in the literature. We believe that the data obtained will facilitate the recognition of the morphological structures of the heart and help researchers who work with SEM.

Acknowledgments

This study is part of a doctoral thesis supported by TÜBİTAK (Project No: 118O758).

Conflict of interest

The authors state that there is no conflict of interest.

10. Nabipour A. Comparative histological structure of the sinus node in mammals. *Turkish Journal of Veterinary and Animal Sciences* 2012; 36 (5): 463-469. doi: 10.3906/vet-0807-2
11. Sanchez-Quintana D, Anderson RH, Cabrera JA, Climent V, Martin R et al. The terminal crest: morphological features relevant to electrophysiology. *Heart* 2002; 88 (4): 406-411. doi: 10.1136/heart.88.4.406
12. Mandrioli D, Ceci F, Balbi T, Ghimenton C, Pierini G. SEM, TEM, and IHC analysis of the sinus node and its implications for the cardiac conduction system. *Anatomy Research International* 2013; 2013: 1-6. doi: 10.1155/2013/961459
13. Nabipour A. A concise review on the anatomy of the atrioventricular node in mammals. *Iranian Journal of Veterinary Science and Technology* 2009; 1 (1): 1-10.
14. Ono N, Yamaguchi T, Ishikawa H, Arakawa M, Takahashi N. Morphological varieties of the purkinje fiber network in mammalian hearts, as revealed by light and electronmicroscopy. *Archives of Histology and Cytology* 2009; 72 (3): 139-149. doi: 10.1679/aohc.72.139
15. Sommer JR, Johnson EA. A comparative study of purkinje fibers and ventricular fibers. *The Journal of Cell Biology* 1968; 36 (3): 497. doi: 10.1083/jcb.36.3.497
16. Kanzaki Y, Terasaki F, Okabe M, Fujita S, Katashima T et al. Three-dimensional architecture of cardiomyocytes and connective tissue in human heart revealed by scanning electron microscopy. *Circulation* 2010; 122 (19): 1973-1974. doi: 10.1161/CIRCULATIONAHA.110.979815
17. Okabe M, Kanzaki Y, Shimomura H, Terasaki F, Hayashi T et al. Back scattered electron imaging: a new method for the study of cardiomyocyte architecture using scanning electron microscopy. *Cardiovascular Pathology* 2000; 9 (2): 103-109. doi: 10.1016/s1054-8807(00)00028-4
18. Myklebust R, Dalen H, Saetersdal TS. A comparative study in the transmission electron microscope and scanning electron microscope of intracellular structures in sheep heart muscle cells. *Journal of Microscopy* 1975; 105 (1): 57-65. doi: 10.1111/j.1365-2818.1975.tb04036.x
19. Perde FV, Atkinson A, Yanni J, Dermengiu D, Dobrzynski H. Morphological characteristics of the sinus node on postmortem tissue. *Folia Morphologica* 2016; 75 (2): 216-223. doi: 10.5603/FM.a2015.0087
20. Duan D, Yu S, Cui Y, Li C. Morphological study of the atrioventricular conduction system and purkinje fibers in yak. *Journal of Morphology* 2017; 278 (7): 975-986. doi: 10.1002/jmor.20691
21. Marino TA. A scanning electron microscopic study of the atrioventricular bundle of the ferret. *Cell and Tissue Research* 1980; 206 (2): 271-277. doi: 10.1007/BF00232771
22. Sanchez-Quintana D, Picazo-Angelín B, Cabrera A, Murillo M, Cabrera JÁ. Koch's triangle and the atrioventricular node in Ebstein's anomaly: implications for catheter ablation. *Revista Española de Cardiología* 2010; 63 (6): 660-667. doi: 10.1016/s1885-5857(10)70140-7
23. Machida N, Katsuda S, Kobayashi Y, Mitsumori KA. Histological study of the cardiac conduction system in a heifer with complete atrioventricular block. *The Journal of Pathology* 2005; 133 (1): 68-72. doi: 10.1016/j.jcpa.2004.12.004
24. Morse DE, Hamlett WC, Noble Jr CW. Morphogenesis of chordae tendineae I: scanning electron microscopy. *The Anatomical Record* 1984; 210 (4): 629-638. doi: 10.1002/ar.1092100410
25. Gauvin R, Marinov G, Mehri Y, Klein J, Li B et al. A comparative study of bovine and porcine pericardium to high light their potential advantages to manufacture percutaneous cardiovascular implants. *Journal of Biomaterials Applications* 2013; 28 (4): 552-565. doi: 10.1177/0885328212465482
26. Jaiswal S, Singh I, Mahanta D, Sathapathy S, Mrigesh M et al. Histological, histomorphometrical, histochemical and ultrastructural studies on the heart of Uttara fowl. *Journal of Entomology and Zoology Studies* 2017; 5 (6): 2365-2370.
27. Saunders R, Amoroso M. SEM investigation of heart tissue samples. *Journal of Physics: Conference Series* 2010; 241 (1): 12-23. doi: 10.1088/1742-6596/241/1/012023
28. Brazile B, Wang B, Wang G, Bertucci R, Prabhu R et al. On the bending properties of porcine mitral, tricuspid, aortic, and pulmonary valve leaflets. *Journal of Long-Term Effects of Medical Implants* 2015; 25: 1-2. doi: 10.1615/jlongtermeffmedimplants.2015011741
29. Dohmen PM, Ozaki S, Nitsch R, Yperman J, Flameng W et al. A tissue engineered heart valve implanted in a juvenile sheep model. *Medical Science Monitor* 2003; 9 (4): 97- 104.
30. Hurler JM, Colvee E, Fernandez-Teran MA. The surface anatomy of the human aortic valve as revealed by scanning electron microscopy. *Anatomy and Embryology* 1985; 172 (1): 61-67. doi: 10.1007/BF00318944
31. Icardo JM, Arrechdera H, Colvee E. The atrioventricular valves of the mouse I. a scanning electron microscope study. *Journal of Anatomy* 1993; 182: 87.
32. Markby G, Summers KM, MacRae VE, Del-Pozo J, Corcoran BM. Myxomatous degeneration of the canine mitral valve: from gross changes to molecular events. *Journal of Comparative Pathology* 2017; 156 (4): 371-383. doi: 10.1016/j.jcpa.2017.01.009
33. Bozzola JJ, Russell LD. *Electron Microscopy Principles and Techniques for Biologist*. 2nd ed. Massachusetts, MA, USA: Jones and Bartlett Publishers; 1998.
34. Choudhary OP, Choudhary P. Scanning electron microscope: advantages and disadvantages in imaging components. *International Journal of Current Microbiology and Applied Sciences* 2017; 6 (5): 1877-1882. doi: 10.20546/ijcmas.2017.605.207
35. Luna LG. *Manual of Histological Staining Methods of the Armed Forces Institute of Pathology*. 3th ed. Newyork, NY, USA: McGraw-Hill Book Company; 1968.

36. Eurell JA, Frappier BL. Dellmann's Textbook of Veterinary Histology. 6th ed. Iowa, IA, USA: Blackwell Publishing; 2006.
37. Leeson CR, Leeson TS, Poporo AA. (1985) Textbook of Histology. 5th ed. Canada, USA: W.B Saunders Company; 1985.
38. Bacha WJ, Bacha LM. Color Atlas of Veterinary Histology. 3rd ed. Chichester, WS, UK: John Wiley& Sons Ltd; 2012.
39. Shimada T, Nakamura M, Kitahara Y, Sachi M. Surface morphology of chemically-digested purkinje fibers of the goat heart. *Journal of Electron Microscopy* 1983; 32 (3): 187-196.
40. Shimada T, Nakamura M, Notohara A. The Purkinje fiber-myocardial cell region in the goat heart as studied by combined scanning electron microscopy and chemical digestion. *Experientia* 1984; 40 (8): 849-850. doi: 10.1007/BF01951989
41. Canale E, Campbell GR, Uehara Y, Fujiwara T, Smolich JJ. Sheep cardiac purkinje fibers: configurational changes during the cardiac cycle. *Cell Tissue* 1983; 232 (1): 97-110. doi: 10.1007/BF00222376
42. Ye X, Bhushan B, Zhou M, Lei W. The surface microstructure of cusps and leaflets in rabbit and mouse heart valves. *Beilstein Journal of Nanotechnology* 2014; 5 (1): 622-629. doi: 10.3762/bjnano.5.73
43. Polliack A, Fu SM, Douglas SD, Bentwich Z, Lampen N et al. Scanning electron microscopy of human lymphocyte-sheep erythrocyterosettes. *Journal of Experimental Medicine* 1974; 140(1): 146-158. doi: 10.1084/jem.140.1.146
44. Polliack A, Lampen N, Clarkson BD, De Harven E, Bentwich Z et al. Identification of human B and T lymphocytes by scanning electron microscopy. *Journal of Experimental Medicine* 1973; 138(3): 607-624. doi: 10.1084/jem.138.3.607